Application of Volterra Series to Ultrasound Imaging

M. Schiffner, M. Mleczko, G. Schmitz
Institute of Medical Engineering, Ruhr-University Bochum, Germany, Email: martin.schiffner@rub.de

Introduction

Diagnostic ultrasound imaging (DUSI) is a real-time imaging modality which provides anatomic and, by the administration of targeted ultrasound contrast agents (UCA), also molecular imaging capabilities. UCA consist of encapsulated gas-filled microbubbles with mean diameters ranging between 1 – 6 µm [1]. In ultrasound pressure fields, the microbubbles demonstrate nonlinear volume oscillations which give rise to harmonics of the fundamental frequency of the incident sound wave in the scattered sound [1, 2]. In general, also wave propagation in tissue is nonlinear and must be taken into account.

Sophisticated physical models exist for both, microbubble oscillations as well as nonlinear wave propagation. They are usually given in terms of nonlinear differential equations. However, current strategies for UCA detection, e. g. phase inversion imaging [3], harmonic imaging [4] or pulse subtraction imaging [5], neglect those and rely on simple mathematical descriptions. These encompass characteristic curves or black box operators accounting only for general properties of a system, e. g. nonlinearity. One major reason for these simplifications is the lack of an intuitive, well-interpretable and manageable means to model nonlinear effects.

This contribution recommends Volterra series as a tool to solve nonlinear differential equations and to describe the nonlinear effects encountered in DUSI with sufficient accuracy. As an example, a solution to the Burgers equation [6] for nonlinear dissipative plane wave propagation outside thermoviscous boundary layers will be derived analytically in terms of a Volterra series. Its region of convergence will be investigated and results of its experimental validation will be presented. An application of Volterra series to pulse subtraction imaging [5] will emphasize the capabilities of nonlinear system theory in state-of-the-art ultrasound imaging.

Functional Description of Nonlinear Systems by Volterra Series

Volterra series can describe the input-output relations of a huge subset of nonlinear systems analytically. They are a generalization of the Taylor series expansion of a function and were first studied by Vito Volterra in the 1880s [7]. The first application of Volterra series to nonlinear system theory was by Norbert Wiener [8].

Let $t \in \mathbb{R}$ denote time in seconds and let $x : \mathbb{R} \mapsto \mathbb{R}$ as well as $h_n : \mathbb{R}^n \mapsto \mathbb{R}$, $n \in \mathbb{N}$, indicate real functions. The system with the input-output relation

$$\begin{aligned} y_n(t) &= \mathrm{H}_n\big[x(t)\big] \\ &= \int \cdots \int_{\mathbb{R}^n} h_n(\nu_1, \ldots, \nu_n) x(t-\nu_1) \cdots \\ &\qquad \times x(t-\nu_n) d\nu_1 \cdots d\nu_n \end{aligned} \tag{1}$$

is then called a time-invariant homogeneous system of degree n [9]. According to [8], the operator H_n is referred to as homogeneous Volterra operator of order n and h_n is its associated Volterra kernel. The additive parallel connection of an infinite number of time-invariant homogeneous systems of distinct degrees yields a Volterra system whose input-output relation

$$y(t) = \mathrm{H}\big[x(t)\big] = \sum_{n=1}^{\infty} \mathrm{H}_n\big[x(t)\big] \tag{2}$$

is described by a Volterra series [9]. The operator H will be referred to as Volterra operator in the sequel. It will be also employed to identify a Volterra system with the input-output relation (2). Since the integrals in (1) resemble n-dimensional convolutions, the Volterra series (2) can be interpreted as a power series in x with memory.

Discontinuous input-output relations as well as input-output relations which exhibit saturation effects cannot be modeled exactly by Volterra series [10].

Analytical Solution to the Burgers Equation

The combined influences of nonlinearity and dissipation on the propagation of plane progressive sound waves can be predicted by the Burgers equation [6]. Its domain of validity includes only nonreacting, weakly thermoviscous fluids and excludes thermoviscous boundary layers. Let p indicate the acoustic pressure, ρ_0 ambient mass density, c_0 small-signal sound speed, β the coefficient of nonlinearity, and δ sound diffusivity. The Burgers equation for sound propagation along the z-axis is then given by

$$\frac{\partial p(z,\tau)}{\partial z} - \frac{\delta}{2{c_0}^3} \frac{\partial^2 p(z,\tau)}{\partial \tau^2} = \frac{\beta}{\rho_0 {c_0}^3} p(z,\tau) \frac{\partial p(z,\tau)}{\partial \tau}, \tag{3}$$

where $\tau = t - z{c_0}^{-1}$ denotes the retarded time.

An innovative analytical solution to a strongly modified version of the Burgers equation for the special case of nonlinear plane wave propagation in cylindrical ducts employing a parameter-dependent Volterra operator was introduced in [11]. It allows for losses induced by thermoviscous boundary layers. However, the same approach can also be adopted to solve (3).

In the following, the parameter-dependent Volterra system $\mathrm{H}^{(\Delta z)}$ is assumed to account for plane wave propagation according to (3). It maps the acoustic pressure $p(z_1,\tau)$ into the acoustic pressure $p(z,\tau)$ at an arbitrary location $z \geq z_1$. The superscript $\Delta z = z - z_1$ indicates the plane wave's propagation distance. Moreover, it is possible to decompose the Burgers equation (3) into a nonlinear interconnection of four linear time-invariant (LTI) systems, whose output signal vanishes. The input signal to each LTI system is $p(z,\tau)$. Consequently, the output signal of the serial connection illustrated in Figure 1 must vanish, too. For convenience, the physical parameters employed in (3) are replaced by $a = \delta(2{c_0}^3)^{-1}$ and $b = \beta(\rho_0{c_0}^3)^{-1}$.

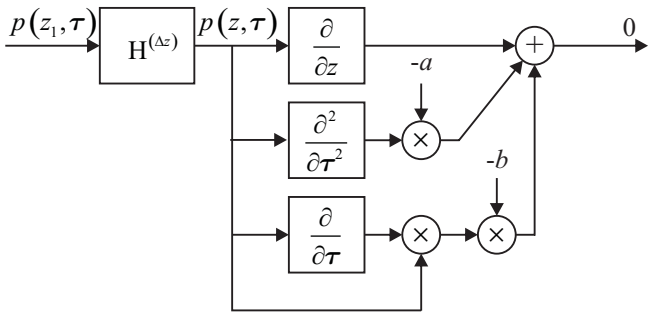

Figure 1: Serial connection of the parameter-dependent Volterra system $\mathrm{H}^{(\Delta z)}$ and the nonlinear interconnection of four LTI systems derived from the Burgers equation (3). The acoustic pressure $p(z_1,\tau)$ is mapped into 0 by the serial connection.

Employing the interconnection theorems for Volterra systems [9] yields the set of ordinary differential equations (ODE)

$$\begin{aligned}\frac{\partial}{\partial z}H_n^{(\Delta z)}(s_1,\ldots,s_n) - a(s_1+\cdots+s_n)^2 H_n^{(\Delta z)}(s_1,\ldots,s_n)\\ = b\sum_{m=1}^{n-1}(s_1+\cdots+s_m)H_m^{(\Delta z)}(s_1,\ldots,s_m)\\ \times H_{n-m}^{(\Delta z)}(s_{m+1},\ldots,s_n)\end{aligned} \tag{4}$$

for the associated Volterra kernels $H_n^{(\Delta z)}$ in Laplace domain, where $s_i = \sigma_i + j\omega_i$, $1 \leq i \leq n$, denote the complex frequencies. Noting the circumstance, that $\mathrm{H}^{(0)}$ is, by definition, the identity operator gives rise to the initial conditions

$$H_n^{(0)}(s_1,\ldots,s_n) = \begin{cases}1 & \text{for } n = 1,\\ 0 & \text{for } n \geq 2.\end{cases} \tag{5}$$

It can be proved by induction, that the unique solution to the set of initial value problems (IVP) (4) and (5) is given by the recurrence relation

$$\begin{aligned}H_n^{(\Delta z)}(s_1,\ldots,s_n) = -\frac{b}{2as_n}\big[H_{n-1}^{(\Delta z)}(s_1,\ldots,s_{n-1})\\ \times H_1^{(\Delta z)}(s_n) - H_{n-1}^{(\Delta z)}(s_1,\ldots,s_{n-2},s_{n-1}+s_n)\big]\end{aligned} \tag{6}$$

for $n \geq 2$, where $H_1^{(\Delta z)}(s_1) = e^{a{s_1}^2\Delta z}$. The Volterra system $\mathrm{H}^{(\Delta z)}$ is completely determined by the knowledge of (6) and $H_1^{(\Delta z)}$. Note that an explicit recurrence relation in terms of Volterra kernels in Laplace domain was not established in [11].

The analytic computation of the corresponding Volterra kernels $h_n^{(\Delta z)}$ in time-domain is trivial only for $n = 1$. The first-order Volterra kernel is the well-known Gauss impulse

$$h_1^{(\Delta z)}(\tau_1) = h_1^{(\Delta z)}(\tau) = \frac{1}{\sqrt{4\pi a\Delta z}}e^{-\frac{\tau^2}{4a\Delta z}}. \tag{7}$$

For $n \geq 2$, the Volterra kernels $h_n^{(\Delta z)}$ can be computed numerically by inverse multidimensional discrete Fourier transforms (DFT) and by considering the sampling theorem.

Normalized versions of the Volterra kernel (7) and the symmetric [9], band-limited Volterra kernel $h_{2,\mathrm{sym,l}}^{(\Delta z)}$ are illustrated in Figure 2 for three propagation distances $\Delta z_1 = 5\,\mathrm{mm}$, $\Delta z_2 = 1\,\mathrm{cm}$, and $\Delta z_3 = 5\,\mathrm{cm}$. The fluid is assumed to be distilled water at ambient temperature $T_0 = 20\,^\circ\mathrm{C}$ and ambient pressure $P_0 = 1013\,\mathrm{hPa}$ ($\rho_0 = 998\,\mathrm{kg\,m^{-3}}$, $c_0 = 1482.87\,\mathrm{m\,s^{-1}}$, $\delta = 4.2514\times10^{-6}\,\mathrm{m^2\,s^{-1}}$, $\beta = 3.5$). To derive $h_{2,\mathrm{sym,l}}^{(\Delta z)}$, two-dimensional 801-samples inverse DFTs at sampling frequency $f_\mathrm{s} = 10\,\mathrm{GHz}$ were employed. The reference values for normalization are

$$h_{1,\mathrm{ref}} = h_1^{(\Delta z_1)}(0) \approx 1.56\times10^8\ \mathrm{s^{-1}}, \tag{8}$$

$$\begin{aligned}h_{2,\mathrm{ref}} &= \max_{-400\leq k_1,k_2\leq 400}\left\{h_{2,\mathrm{sym,l}}^{(\Delta z_1)}[k_1,k_2]\right\}\\ &\approx 2.7\times10^{10}\ \mathrm{Pa^{-1}\,s^{-1}},\end{aligned} \tag{9}$$

for the kernels $h_1^{(\Delta z)}$ and $h_{2,\mathrm{sym,l}}^{(\Delta z)}$, respectively.

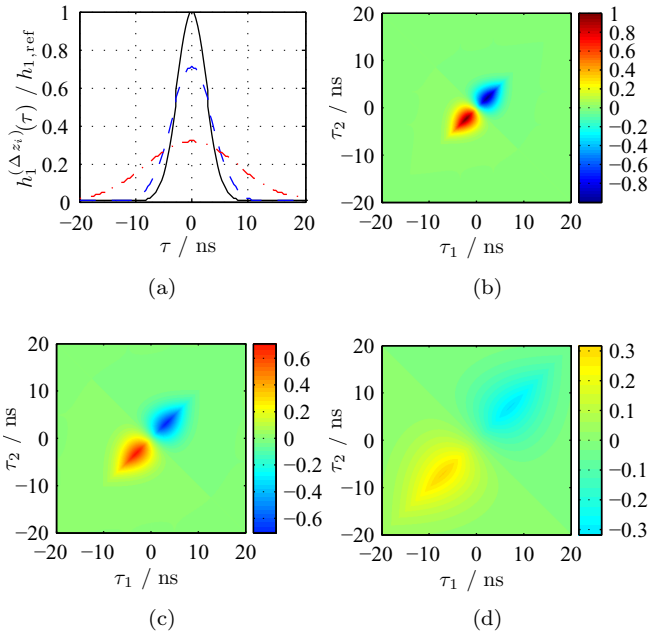

Figure 2: Normalized Volterra kernels $h_1^{(\Delta z_i)}$ (a) and normalized Volterra kernels $h_{2,\mathrm{sym,l}}^{(\Delta z_i)}$ (b – d) for three propagation distances $\Delta z_1 = 5\,\mathrm{mm}$ (solid line, b), $\Delta z_2 = 1\,\mathrm{cm}$ (dashed line, c), and $\Delta z_3 = 5\,\mathrm{cm}$ (dash-dotted line, d).

In consideration of an application of the derived Volterra system $\mathrm{H}^{(\Delta z)}$ in DUSI the investigation of its region of convergence $R_h(\Delta z)$ is mandatory. Convergence of $\mathrm{H}^{(\Delta z)}$ implies bounded-input, bounded-output (BIBO) stability for acoustic pressures satisfying

$$\big\|p(z_1,\tau)\big\|_\infty = \max_{\tau\in\mathbb{R}}\Big\{\big|p(z_1,\tau)\big|\Big\} < R_h(\Delta z).$$

Again, a common approach as used in [11] can be adopted. It is assumed, that there exist $g_{\Delta z} > 0$, $K_{\Delta z} > 0$ as well as $n_0 \in \mathbb{N}$, such that the associated Volterra kernels satisfy

$$\begin{aligned}\big\|h_n^{(\Delta z)}\big\|_1 &= \int\cdots\int_{\mathbb{R}^n}\big|h_n^{(\Delta z)}(\tau_1,\ldots,\tau_n)\big|d\tau_1\cdots d\tau_n \\ &\le {K_{\Delta z}g_{\Delta z}}^n < \infty,\end{aligned} \tag{10}$$

for $n \ge n_0$. Additionally, $\|h_n^{(\Delta z)}\|_1 < \infty$ for $1 \le n < n_0$ is required. As a consequence

$$\begin{aligned}\big|p(z,\tau)\big| \le{}& \sum_{n=1}^{n_0-1}\Big|\mathrm{H}_n^{(\Delta z)}\big[p(z_1,\tau)\big]\Big| + \frac{{K_{\Delta z}g_{\Delta z}}^{n_0}\big\|p(z_1,\tau)\big\|_\infty^{n_0}}{1-g_{\Delta z}\big\|p(z_1,\tau)\big\|_\infty} \\ &< \infty\end{aligned}$$

for $g_{\Delta z}\|p(z_1,\tau)\|_\infty < 1$ due to the properties of the geometric series combined with definition (2). Thus, the Volterra series converges absolutely with region of convergence $R_h(\Delta z) = {g_{\Delta z}}^{-1}$.

Taking into account that $\mathrm{H}^{(0)}$ is the identity operator with $R_h(0) \to \infty$, the region of convergence $R_h(\Delta z)$ may be expected to be greater than 1 Pa for several propagation distances $\Delta z > 0$. This circumstance implies $0 < g_{\Delta z} < 1$. Due to the inequalities $|H_n^{(\Delta z)}(j\omega_1,\ldots,j\omega_n)| \le \|h_n^{(\Delta z)}\|_1$ the asymptotic behavior of the Fourier transformed Volterra kernels for $n \gg n_0$ is

$$\big|H_n^{(\Delta z)}(j\omega_1,\ldots,j\omega_n)\big| \approx {K_{\Delta z}g_{\Delta z}}^n. \tag{11}$$

The quotient of the absolute values

$$\begin{aligned}\hat{R}_h^{(\Delta z)}(n) &= \frac{\big|H_n^{(\Delta z)}(j\omega_1,\ldots,j\omega_n)\big|}{\big|H_{n+1}^{(\Delta z)}(j\omega_1,\ldots,j\omega_{n+1})\big|} \\ &\approx \frac{1}{g_{\Delta z}} = R_h(\Delta z)\end{aligned} \tag{12}$$

for $n \gg n_0$ lends itself as an approximation for the region of convergence. If condition (10) is met, the quotient (12) must approach a constant value as n grows. This behavior was observed in numerical computations. Due to the knowledge of the recurrence relation (6), the region of convergence can be approximated for arbitrary values $n \in \mathbb{N}$ by employing (12). In [11] only the first nine Volterra kernels in Laplace domain were used to investigate convergence.

The approximation (12) was computed for propagation distances Δz ranging from 1 mm to 5 cm for $n = 10^3$. To avoid singularities and for convenience all angular frequencies $\omega_1,\ldots,\omega_{n+1}$ in (12) were identically set to $\omega_{0,j} = 2\pi f_{0,j}$. Mathematically, the choice of $\omega_{0,j}$ is arbitrary and does not influence the asymptotic behavior (11). Four different values $f_{0,j}$ were employed. The corresponding results are illustrated in Figure 3 (dashed lines). The curves differ due to the finite order $n = 10^3$. Their minimal values (solid line) are assumed to indicate the true region of convergence. As before, the fluid is distilled water at identical environmental conditions.

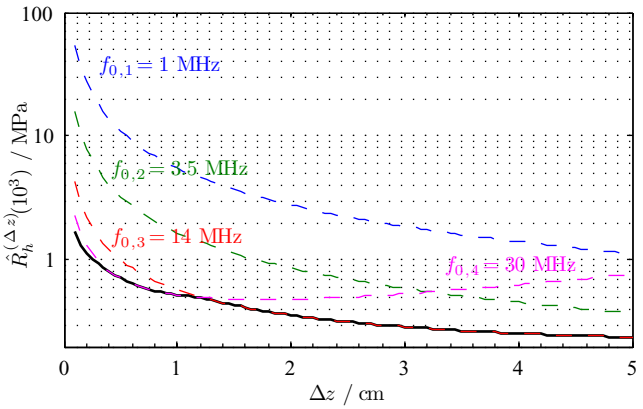

Figure 3: Approximation (12) for propagation distances Δz in the range from 1 mm to 5 cm for $n = 10^3$.

The derived Volterra series was validated experimentally. The degree-2 Volterra polynomial was combined with the angular spectrum approach, which accounts for linear diffraction effects according to the Helmholtz equation, in a second-order fractional steps scheme, as presented in [12]. A 1.27 cm diameter transducer (Panametrics-NDT C306) spherically focused at 45 mm and submerged in distilled water at $T_0 = 20\,^\circ\mathrm{C}$ was employed for measurements. Its center frequency was $f_\mathrm{c} = 2.25$ MHz. After eleven succeeding propagation steps of length 5 mm the relative error between the calculated and measured waveforms was smaller than 20 % for acoustic pressures up to 1 MPa and smaller than 15 % for acoustic pressures up to 500 kPa. Only waveforms along the transducer's axis were considered. Volterra polynomials of higher degrees did not yield different results for propagation steps of length 5 mm.

Consequently, the application of the derived Volterra series in DUSI is appropriate. The following section will demonstrate the advantages of nonlinear system theory in the interpretation and optimization of pulse subtraction imaging.

Application to Pulse Subtraction Imaging

In pulse subtraction imaging three excitation signals x_1, x_2, and x_3 are utilized [5]. For $t_1 < t_2 < t_3$ they must satisfy

$$\begin{aligned} x_1(t) &= 0 && \text{for } t \le t_1 \wedge t > t_2, \\ x_2(t) &= 0 && \text{for } t \le t_2 \wedge t > t_3, \\ x_3(t) &= x_1(t) + x_2(t) && \text{for } t \in \mathbb{R}. \end{aligned} \tag{13}$$

Except for the requirements (13) the choice of x_1 and x_2 is arbitrary.

Employing the operator G to model the signal chain of a DUSI system, the following operation is performed on the corresponding received signals $\mathrm{G}\big[x_j(t)\big]$

$$\chi(t) = \mathrm{G}\big[x_3(t)\big] - \mathrm{G}\big[x_1(t)\big] - \mathrm{G}\big[x_2(t)\big]. \qquad (14)$$

For a Volterra operator G describing an LTI system ($g_n = 0$ for $n \geq 2$) or a memoryless system ($g_n(t_1, \ldots, t_n) = \alpha_n \delta(t_1, \ldots, t_n)$, $\alpha_n \in \mathbb{R}$) the residual signal χ vanishes. This circumstance was demonstrated in [5]. However, for a general Volterra operator G with the associated symmetric kernels $g_{n,\mathrm{sym}}$ the residual signal results in

$$\begin{aligned}\chi(t) = &\sum_{n=2}^{\infty} \sum_{j=1}^{n-1} \binom{n}{j} \int \cdots \int_{\mathbb{R}^n} g_{n,\mathrm{sym}}(\nu_{j,1}^{(n)}, \ldots, \nu_{j,n}^{(n)}) \\ &\times \prod_{i=1}^{n-j} x_1(t - \nu_{j,i}^{(n)}) \prod_{i=n-j+1}^{n} x_2(t - \nu_{j,i}^{(n)}) \qquad (15) \\ &\times d\nu_{j,1}^{(n)} \cdots d\nu_{j,n}^{(n)}.\end{aligned}$$

Due to (13), the product terms within the integrals (15) are nonzero only for certain relationships between the integration variables $\nu_{j,i}^{(n)}$. Let $I_{n,1}(j) = \{1, \ldots, n-j\}$ and $I_{n,2}(j) = \{n-j+1, \ldots, n\}$ for $1 \leq j \leq n-1$, then for each order $n \geq 2$ the $n-1$ sets of inequalities

$$\begin{aligned} |\nu_{j,k}^{(n)} - \nu_{j,l}^{(n)}| &< t_2 - t_1 \quad \text{for } k, l \in I_{n,1}(j), \\ |\nu_{j,m}^{(n)} - \nu_{j,p}^{(n)}| &< t_3 - t_2 \quad \text{for } m, p \in I_{n,2}(j), \qquad (16) \\ 0 < \nu_{j,k}^{(n)} - \nu_{j,m}^{(n)} &< t_3 - t_1 \quad \text{for } k \in I_{n,1}(j) \wedge m \in I_{n,2}(j) \end{aligned}$$

must be met for (15) to be nonzero. Note that the sets (16) are not satisfied for $\nu_{j,1}^{(n)} = \cdots = \nu_{j,n}^{(n)}$. Thus, the residual signal (15) vanishes also for Volterra operators G, whose associated symmetric kernels have support only on their diagonals. These kernels arise in serial connections of static nonlinear systems preceding LTI systems.

As illustrated in Figure 2 the second-order Volterra kernels for nonlinear wave propagation are sparse. They are mainly occupied along their diagonals. Mleczko et al. demonstrated in [13] that Volterra kernels identified from a free microbubble do not share this property. Thus, (15) serves as a starting-point for further optimizations. The goal is to find the Volterra kernels $g_{n,\mathrm{sym}}$ associated to the complete signal chain of a DUSI system for both cases, with UCA microbubbles present and without their presence. Subsequently, (15) can be tuned to be sensitive towards the case with UCA microbubbles by the choice of the input signals x_1 and x_2.

Conclusion and Outlook

Volterra series are capable to model nonlinear effects encountered in DUSI with sufficient accuracy. A solution to the widely-used Burgers equation in terms of a Volterra series was derived and its region of convergence was investigated. Results of the experimental validation were presented. The application of Volterra series to pulse subtraction imaging [5] yields well-interpretable results, which serve as a starting-point for further optimizations.

References

[1] Postema, M. and Schmitz, G.: Bubble dynamics involved in ultrasound imaging. Exp. Rev. Mol. Imag. **6**(3) (2006), 493–502

[2] de Jong, N., Bouakaz, A., and Frinking, P.: Basic Acoustic Properties of Microbubbles. Echocardiography **19**(3) (2002), 229–240

[3] Simpson, D. H., Chin, C. T., and Burns, P. N.: Pulse Inversion Doppler: A New Method for Detecting Nonlinear Echoes from Microbubble Contrast Agents. IEEE Transactions on Ultrasonics, Ferroelectrics, and Frequency Control **46**(2) (1999), 372–382

[4] Borsboom, J. M. G., Chin, C. T., Bouakaz, A., Versluis, M., and de Jong, N.: Harmonic Chirp Imaging Method for Ultrasound Contrast Agent. IEEE Transactions on Ultrasonics, Ferroelectrics, and Frequency Control **52**(2) (2005), 241–249

[5] Borsboom, J. M. G.: Advanced Detection Strategies for Ultrasound Contrast Agents. Ph.D. thesis, Erasmus Universiteit Rotterdam (2005)

[6] Hamilton, M. F. and Blackstock, D. T., eds.: Nonlinear Acoustics. Academic Press (1997)

[7] Volterra, V.: Theory of Functionals and of Integral and Integro-Differential Equations. Dover Publications, New York (1930)

[8] Schetzen, M.: The Volterra and Wiener Theories of Nonlinear Systems. Krieger Publishing Company, Malabar, Florida, reprint ed. (2006)

[9] Rugh, W. J.: Nonlinear System Theory - The Volterra / Wiener Approach. The John Hopkins University Press, web ed. (2002). Available online: `https://jshare.johnshopkins.edu/wrughii1/public_html/volterraseriesbook.pdf`

[10] Frank, W.: Aufwandsarme Modellierung und Kompensation nichtlinearer Systeme auf der Basis von Volterra-Reihen. Ph.D. thesis, Institut für Mathematik und Datenverarbeitung der Universität der Bundeswehr München (1997)

[11] Hélie, T. and Hasler, M.: Volterra series for solving weakly non-linear partial differential equations: application to a dissipative Burgers' equation. International Journal of Control **77**(12) (2004), 1071–1082

[12] Zemp, R. J., Tavakkoli, J., and Cobbold, R. S. C.: Modeling of nonlinear ultrasound propagation in tissue from array transducers. Journal of the Acoustical Society of America **113**(1) (2003), 139–152

[13] Mleczko, M., Postema, M., and Schmitz, G.: Discussion of the application of finite volterra series for the modeling of the oscillation behavior of ultrasound contrast agents. Appl Acoust (2008), in press, DOI: 10.1016/j.apacoust.2008.09.012